16th World Conference on Earthquake, 16WCEE 2017
Santiago Chile, January 9th to 13th 2017
Paper N° 2057
Registration Code: S-E146191

DYNAMIC STRUCTURE-SOIL-STRUCTURE INTERACTIONS

MODELING AND EXPERIMENTS

C. Boutin, J. Soubestre, L. Schwan, M. Dietz*

ENTPE, Université de Lyon, L GCB/TDS UMR 5513 CNRS, Vaulx-en-Velin, France.
** University of Bristol - UK*

Abstract

The seismic response in presence of multiple interactions between structures through the soil is extremely complex even when the structures and the soil behave linearly. However, two facts reduce the complexity of the problem. First, some structures are built according to a periodic pattern and second, the seismic spectrum generates wavelengths significantly than the characteristic size of the studied system. In this double circumstance, it is possible to address the multiple interactions in the rigorous framework of the homogenisation method.

In this paper, two examples of this approach are considered, namely the dynamics of soft soil layer reinforced by a periodic distribution of piles, and the influence of the city on the seismic response at the settlement sites scale. In both cases the theory is validated by experiments on analogous specimens performed on a shaking table (European project SERIES).

The soil with piles is treated as a composite made of a soft matrix - the soil, working in shear as usual - periodically reinforced by linear slender elastic inclusions, i.e. the piles considered as beams and thus working in bending. It is shown that the overall behaviour of such a system couples the shear and bending effects, with simple expressions of the effective parameters. The experiments comfort this theoretical modelling. These results make questionable the usual description based on Winkler model, where the soil is assumed to react in extension-compression (with parameters adjusted in a empirical way).

The seismic response of a densely urbanized city resting on a homogeneous plane half space is studied in an idealized situation : the city is seen a periodic distribution of linear oscillator describing the first eigen mode of the buildings. The homogenisation analysis shows that the city behaves as a resonating surface characterized by an impedance, whose the properties are inherited from that of the oscillators. This enables simple parametric studies of the actual city effects on the ground motions. The experimental program conducted on a set of 37 oscillators lying on an elastic layer provides results in accordance with the theoretical city impedance model. Direct engineering applications concern the effective impedance of groups of few (say more than 5) similar buildings.

Keywords Homogenization ; Dynamics ; Pile foundations ; Soil-structure interaction ; Site-city effect.

1. Introduction

In earthquake engineering, the "exact" treatment of the seismic response in presence of multiple interactions between structures through the soil is extremely complex even when the structure and soil behaviours are assumed linear, as usual in geophysics and structural dynamics. However, we can take benefit of two facts to reduce the complexity of the problem. First, some structures are built according to a periodic design (of few meters length) and second, the seismic spectrum generates wavelengths significantly larger (say 5 to 10 times) than the characteristic size of the studied system. When this condition of scale separation is fulfilled one may use the classical framework of two scale asymptotic homogenisation method [1, 2], to derive the global behaviour.

Two examples of this approach are addressed in the sequel, namely the dynamics of soft soil layer reinforced by a periodic distribution of piles and the influence of the city on the seismic response at the settlement sites scale. The analysis proceeds by scale change from the pile and soil period to the reinforced layer in the first case, and from the building scale to the global city scale in the second case. In both cases the theoretical approach is completed by a validation by experiments on analogous specimens performed on a shaking table.

2. Dynamics of soils reinforced by piles

The dynamic pile-soil-pile interaction is of importance in earthquake engineering [3]. However, in practice the numerical treatment is ill conditioned and the problem remains in general an open question. The soil with piles is here considered as a composite made of a soft matrix (soil, working in shear as usual) periodically reinforced by linear slender elastic inclusions (piles considered as beam and thus working in bending), [4].

2.1. Setting of the problem

Consider an homogeneous soil matrix (index m) in which a periodic array of parallel identical homogeneous straight piles (index p) is embedded with a perfect contact (Fig. 1).

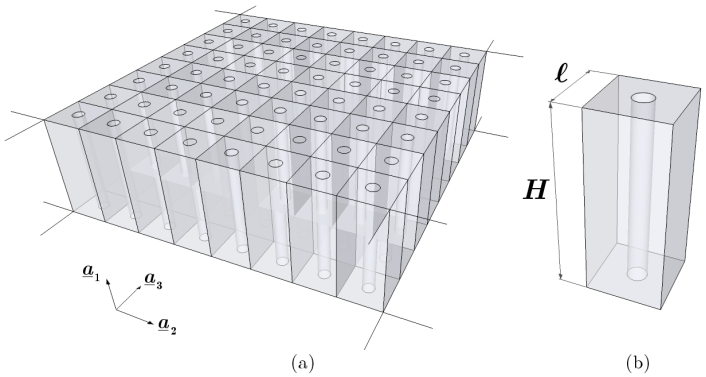

Fig. 1. Soil matrix (index m) and piles (index p) periodic system.

The characteristic size of the period (square or rectangle) is l.

The soil and the pile are assumed to have an isotropic linear elastic behaviour characterized by their Lame coefficients λ_q and μ_q ($q = m, p$) or Young's modulus E_q and Poisson's ratio ν_q. Their density are denoted by ρ_q. The media presents a 2D-period S : $S = S_p \cup S_m$, where S_p stands for the pile section and S_m for the soil section. The interface between the two constituents is denoted Γ. The pile concentration of beams is $c = |S_p|/|S|$. The local problems are set on the frame originated at the center of mass of the pile section and orientated along its principal inertia axis. We denote by I_α the pile section inertia in the principal direction $\underline{a}_\alpha$. The axial dimension of the piles, H, is much larger than the lateral dimension l of the period. We are interested in identifiying the

global behaviour of the soil-piles system, relevant for deformation phenomena varying according to a macroscopic length L, much larger than l. This introduce scale parameter used in the asymptotic expansions

$$\varepsilon = l/L \ll 1$$

The geometry specifies the axial direction (of unit vector a_1) and the directions in the plane of the section (of unit vectors a_α, $\alpha = 2,3$). Herein, Greek indices run from 2 to 3 and Latin ones from 1 to 3. The relevant dimensionless space variables are $(x_i/L, x_\alpha/l)$ and the appropriate physical space variables are (x_i, y_α), where $y_\alpha = \varepsilon^{-1} x_\alpha$. Thus, any function $f(x_i)$ is rewritten as $f(x_i, y_\alpha)$ and its gradient becomes $\partial f/\partial x_i \; a_i + \varepsilon^{-1} \partial f/\partial y_\alpha \; a_\alpha$. According to the scale separation and to the in-plane periodic geometry, the variables are S-periodic. Hence, the displacements in both constituents (pre-exponent $q = m, p$) are looked for in the form

$$^q u = {}^q u_j(x_i, y_\alpha) a_j \qquad \text{with} \quad {}^m u \; S\text{–periodic in } y_\alpha.$$

Using the asymptotic process, motions in both constituents ($q = m, p$) are looked for in the form of two-scale expansions in powers of ε:

$$^q \underline{u} = \sum_{k=0}^{\infty} \varepsilon^k \, ({}^q u_j^k(x_i, y_\alpha) \, \underline{a}_j) \qquad \text{with} \qquad {}^m u_j^k(x_i, y_\alpha) \;\; S-\text{periodic in } y_\alpha.$$

The specificity of the axial direction leads to decompose strain tensor ^{q}e, and stress tensor $^q\sigma$ in each constituent ($q = m, p$) - into three reduced tensors ($\otimes$ stands for the tensorial product) :

$$A = A_n \, a_1 \otimes a_1 + (A_t \otimes a_1 + a_1 \otimes A_t) + A_s \qquad \text{where} \qquad A = \text{e or } A = \sigma;$$

- $A_n = A_{11}$: *scalar axial* strain or stress;
- $A_t = A_{1\alpha} \, a_\alpha$: 2D strain or stress *vector* exerted *out of the plane* of the section;
- $A_s = A_{\alpha\beta}/2 \; (a_\alpha \otimes a_\beta + a_\beta \otimes a_\alpha)$: strain or stress *tensor in the plane* of the section.

By using the x,y-formulation, these tensors read (where Is $= a_2 \otimes a_2 + a_3 \otimes a_3$):

$$\begin{array}{lll} e_n = u_{1,x_1} & ; & \sigma_n = 2\mu e_n + \lambda(\mathrm{tr}(\underline{\underline{e}}_s) + e_n) \\ \underline{e}_t = [(\varepsilon^{-1} u_{1,y_\alpha} + u_{1,x_\alpha} + u_{\alpha,x_1})/2]\underline{a}_\alpha & ; & \underline{\sigma}_t = 2\mu \underline{e}_t \\ \underline{\underline{e}}_s = \varepsilon^{-1}[(u_{\alpha,y_\beta} + u_{\beta,y_\alpha})/2](\underline{a}_\alpha \otimes \underline{a}_\beta + \underline{a}_\beta \otimes \underline{a}_\alpha)/2 & ; & \underline{\underline{\sigma}}_s = 2\mu \underline{\underline{e}}_s + \lambda(\mathrm{tr}(\underline{\underline{e}}_s) + e_n)\underline{\underline{I}}_s \end{array}$$

The beam and matrix dynamic equilibriums in harmonic regime read (as the problem is linear, the term $\exp(i\omega t)$ is omitted to lighten the notations):

$$\left\{ \begin{array}{rcll} \underline{\mathrm{div}}(^q\underline{\underline{\sigma}}) & = & -\rho_q \omega^2 \, {}^q\underline{u} & \text{in } S_q \\ [\underline{\underline{\sigma}} . \underline{n}] = \underline{0} & , & [\underline{u}] = \underline{0} & \text{on } \Gamma \quad ; \quad {}^m\underline{\underline{\sigma}} \;\; S\text{-periodic in } \underline{y} \end{array} \right.$$

where [.] denotes the jump at the interface. This set rewritten with (x_i, y_α) splits into :

- scalar equations expressing the axial balance (along a_1)

$$\left\{ \begin{array}{rcll} \varepsilon^{-1} \mathrm{div}_y(^q\underline{\sigma}_t) + \mathrm{div}_x(^q\underline{\sigma}_t) + \dfrac{\partial \, {}^q\sigma_n}{\partial x_1} & = & -\rho_q \omega^2 \, {}^q u_1 & \text{in } S_q, \;\; q = m, p \\ [\underline{\sigma}_t . \underline{n}] = 0 & , & [u_1] = 0 & \text{on } \Gamma \quad ; \quad {}^m\underline{\sigma}_t \;\; S\text{-periodic in } \underline{y} \end{array} \right.$$

- vectorial sets expressing the in-plane balance (within (a_2, a_3))

$$\left\{\begin{array}{rcll} \varepsilon^{-1}\,\underline{\mathrm{div}}_y({}^q\underline{\underline{\sigma}}_s)+\underline{\mathrm{div}}_x({}^q\underline{\underline{\sigma}}_s)+\dfrac{\partial\,{}^q\underline{\sigma}_t}{\partial x_1} & = & -\rho_q\,\omega^2\,u_\alpha\,\underline{a}_\alpha & \text{in } S_q,\ q=m,p \\ [\underline{\underline{\sigma}}_s.\underline{n}]=\underline{0} \quad , \quad [u_\alpha\underline{a}_\alpha]=\underline{0} & & & \text{on } \Gamma \quad ; \quad {}^m\underline{\underline{\sigma}}_s \ S\text{-periodic in } \underline{y} \end{array}\right.$$

The contrast of mechanical properties between the soil and the piles plays a crucial role: without soil, the pile array would be governed by bending; while if the soil and the piles stiffnesses were identical, the behaviour would be governed by shear. A coupling between shear in the soil and bending in the beams are derived from a dimensional analysis, occurs when the piles modulus is of the order of the square of the slender ratio (of the pile) compared to the shear modulus of the soil. Hence, we focus on media presenting a ε^2 stiffness contrast, i.e. (the notation $O(.)$ stand for "of the order of") :

$$\mu_m = O(\varepsilon^2\mu_p) = \varepsilon^2\mu'_m \quad \text{and} \quad \lambda_m = O(\varepsilon^2\lambda_p) = O(\varepsilon^2\lambda'_m)$$

and the stresses in both constituents are written in the form below:

$$\sigma_p = \lambda_p\,\mathrm{tr}(\mathrm{e}_p)\mathrm{I} + 2\mu_p\mathrm{e}_p \qquad \sigma_m = \varepsilon^2(\lambda'_m\mathrm{tr}(\mathrm{e}_m)\mathrm{I} + 2\mu'_m\mathrm{e}_m)$$

In both constituents, problems at different orders are obtained by introducing the asymptotic expansions into the dynamic balance equations. This problems are solved successively until the macroscopic description is obtained.

2.2 Transverse dynamic behaviour

Focusing on transverse kinematics, one derives, [5], the following leading order in-plane balance equations (where $\{i\,j\} = \{11, 22, 33, 23\}$) :

$$\underline{\mathrm{div}}_x\left(\langle\underline{\tilde{\sigma}}^2_t\rangle\otimes\underline{a}_1+\langle\underline{\tilde{\underline{\sigma}}}^2_s\rangle\right) = -\langle\rho\rangle\,\omega^2\,U^0_\alpha\,\underline{a}_\alpha$$

$$\langle\underline{\tilde{\sigma}}^2_t\rangle\otimes\underline{a}_1+\langle\underline{\tilde{\underline{\sigma}}}^2_s\rangle = \left(C^{1\beta}_{1\alpha}\,\mathrm{e}_{x1\beta}(\underline{U}^0)-E_p\,\frac{I_{p\alpha}}{|S|}\,\frac{\partial^3 U^0_\alpha}{\partial x_1^3}\right)\underline{a}_\alpha\otimes\underline{a}_1+C^{ij}_{\alpha\beta}\,\mathrm{e}_{xij}(\underline{U}^0)\,\underline{a}_\alpha\otimes\underline{a}_\beta$$

where here and in the sequel we denote the average by the notation :

$$\langle . \rangle = \frac{1}{S_m}\int_{S_m} . ds + \frac{1}{S_p}\int_{S_p} . ds$$

This set expresses the dynamics associated with the transverse kinematics. A bending effect is involved at the leading order when the transverse component U_α presents an x_1-axial variation. The coefficients of the elastic tensor C are identical to those of the elastic matrix reinforced by perfectly rigid inclusion (occupying the beam domain). As for inertia, the equivalent density is the mean density as in classic dynamics of elastic composites. In quasi-static regime, this second gradient model is of the same nature as the model established by [6] and simplifies the bi-phasic developed by [7].

This description enables to investigate the homogenous transverse modes - in the form $U^0_\alpha(x_1)a_\alpha$ - of a reinforced layer of finite thickness H (and bi-symmetric matrix/beam period so that C is transverse isotropic), [5]. By considering, for simplicity, motions in the direction a and by using the lightened notations $U^0 = U$; $x_1 = x$; $I_{p2} = I_p$; $C_{12} = 2G$, the equilibrium condition reduces to the scalar equation :

$$-\frac{E_p\,I_p}{|S|}\,\frac{d^4U}{dx^4}+G\,\frac{d^2U}{dx^2}+\langle\rho\rangle\,\omega^2\,U=0$$

Denoting by δ_1 and δ_2 the roots of the associated characteristic equation, the general solution is in the form

$$U(x) = a\,\mathrm{ch}\left(\delta_2\,\frac{x}{H}\right)+b\,\mathrm{sh}\left(\delta_2\,\frac{x}{H}\right)+c\cos\left(\delta_1\,\frac{x}{H}\right)+d\sin\left(\delta_1\,\frac{x}{H}\right)$$

$$\delta_1^2\,\delta_2^2 = \frac{\omega^2\,|S|\,\langle\rho\rangle\,H^4}{E_p\,I_p} \quad ; \quad \delta_2^2-\delta_1^2 = \frac{G\,|S|\,H^2}{E_p\,I_p} = K$$

where the dimensionless parameter K weighs the bending effects compared to shear effects. Bending predominates when K is small, shear when K is large. The boundary conditions must be specified at the bottom ($x = 0$) and top ($x = H$) of the layer. Due to the second gradient/bending effect, four types of simple boundary conditions are possible: (i) Free, i.e. zero shear force, zero momentum ; (ii) Clamped, i.e., zero translation U, zero rotation U' ; (iii) Articulated i.e. zero translation, zero momentum and (iv) Sliding i.e. zero rotation, zero shear force. They reads explicitly :

- Free condition (denoted L): $\langle \tilde{\sigma}_t^2 \rangle = GU' - E_p I_p / |S| \, U''' = 0 \quad \text{and} \quad U'' = 0,$
- Clamped condition (denoted E): $U = 0 \quad \text{and} \quad U' = 0,$
- Articulated condition (denoted A): $U = 0 \quad \text{and} \quad U'' = 0,$
- Sliding condition (denoted G): $\langle \tilde{\sigma}_t^2 \rangle = GU' - E_p I_p / |S| \, U''' = 0 \quad \text{and} \quad U' = 0.$

The modal analysis is performed for different boundary conditions (the first and second conditions are related to the bottom ($x = 0$) and top ($x = H$)) : clamped-free (EL), clamped-sliding (EG), articulated-sliding (AG) and articulated-free (AL). These conditions lead to a set of four linear equations and the modes correspond to the non trivial solutions obtained when the determinant vanishes. This results in the following modal equations:

- Clamped-Free : $\dfrac{K}{\delta_1^2 \delta_2^2} + \dfrac{\text{th}(\delta_2)\tan(\delta_1)}{\delta_1 \delta_2} + \dfrac{2}{K}\left(1 + \dfrac{1}{\cos(\delta_1)\text{ch}(\delta_2)}\right) = 0$
- Clamped-Sliding : $\delta_1 \tan(\delta_1) + \delta_2 \, \text{th}(\delta_2) = 0$
- Articulated-Sliding : $\cos(\delta_1) = 0$
- Articulated-Free : $\delta_2^3 \, \text{th}(\delta_2) - \delta_1^3 \tan(\delta_1) = 0$

For each case, the modal equation can be solved numerically as a function of K to derive the solutions δ_{1i} and δ_{2i} corresponding to the i^{th} mode. Eigen frequencies and mode shapes of the reinforced layer can then be derived.

(a) (b)

Fig. 2. Physical model of reinforced soil fixed on the shaking table. (a) Free top boundary condition. (b) Rigid lattice of aluminium bars connected to the top of the fibers enabling the translational top condition.

2.2 Experiments on a physical model

In the frame work of the European project Series, an experimental program has been realized [8] in order to validate the homogenized model. The materials of the physical model were chosen to match the large stiffness contrast between the matrix and the fibers, both being isotropic linear elastic materials and presenting a perfect adherence at their interface. The matrix is a polyurethane foam of density $\rho_m = 48$ kg/m^3 and shear modulus $G_m =$ 24.3 kPa. The fibers are round mild steel seamless tube of modulus $E_p = 210$ GPa, density $\rho_p = 7800$ $kg/m3$, with

diameter and wall thickness of 12.7 *mm* and 3.25 *mm*. The physical model was designed so that both bending and shear mechanisms would occur at resonance. The dimensional analysis of the governing equation gives the following relations in order of magnitude:

$$E_p I_p = O(GSH^2) = O\left(\langle \rho \rangle SH^4 \omega^2\right)$$

The test specimen (Fig. 2-a) has a footprint of 2.13×1.75 m^2. A 25*cm* spacing between fibers permits a reasonable periodicity with 35 fibers giving the surface value S = 0.25×0.25 m^2. With a model height of H = 1.25*m*, the left hand side of the above relation is satisfied while the right hand side gives a fundamental frequency less than 10*Hz*, appropriate for an accurate control of the shaking table. Two concentrations with periodic arrangements were tested, (i) 35 fibers distributed on a 7 by 5 square grid of 25c*m* side, giving a fiber concentration c of 0.2%, (ii) 17 fibers distributed in staggered rows at √2×25c*m* centres, giving c = 0.1%. For both fiber concentration, the four type boundary conditions EL, EG, AL, AG were tested. For clamped-free (EL) conditions, the fibers were bolted to the base-plate. For sliding condition (G) , a rigid lattice was fixed at the top of the fibers to avoid the rotation and allow the translation (Fig. 2-b). The rotational condition (A) at the bottom of the fibers was realized by placing a steel ball between the base-plate and the fiber.

The model is firmly clamped on the table and the shaking table imposes a horizontal uni-directional rigid body motion. The model responds to the motion imposed at its base and its motion is recorded using the sensors. White noise enables identification of the first eigen frequencies (Fig. 3-a). Harmonic sinusoidal motion are used to excite the model at its eigen frequencies for accurate determination of the mode characteristics (Fig. 4-a).

Single-axis accelerometers are mounted on the shaking table, on the uppermost surface of the matrix, on the fiber protruding from the top of the matrix, and a vertical face of the sample. The identical accelerations recorded on the foam and on the fibers indicates that both follow the same horizontal translation motion, as derived by the homogenised model under the assumption of perfect adherence. Further, the accelerometers enable to identify the eigen frequency, and the fundamental mode shape.

Six fibers were instrumented with 3 pairs of longitudinal strain gauges (located (i) at the fiber bottom (B+/-, 38.5*mm* from the base), (ii) at the middle (M+/-, 625*mm* from the base) and (iii) at the top (T+/-, 1211.5 *mm* from the base). The response demonstrated the bending deformation of fibers, according to the nature of the boundary conditions (Fig. 3-b). Since the material properties, the geometry and the boundary conditions of the test specimen are (almost) exactly known, the homogenised model has been used to determine the expected behaviour. The measured fundamental frequencies match the homogenised model ones, with an error of about 1% for clamped-free (EL) boundary conditions (6% for EG condition ; 15% for AL or AG conditions). These values significantly depart form that given the pure bending and the usual composite model (whitout bending).

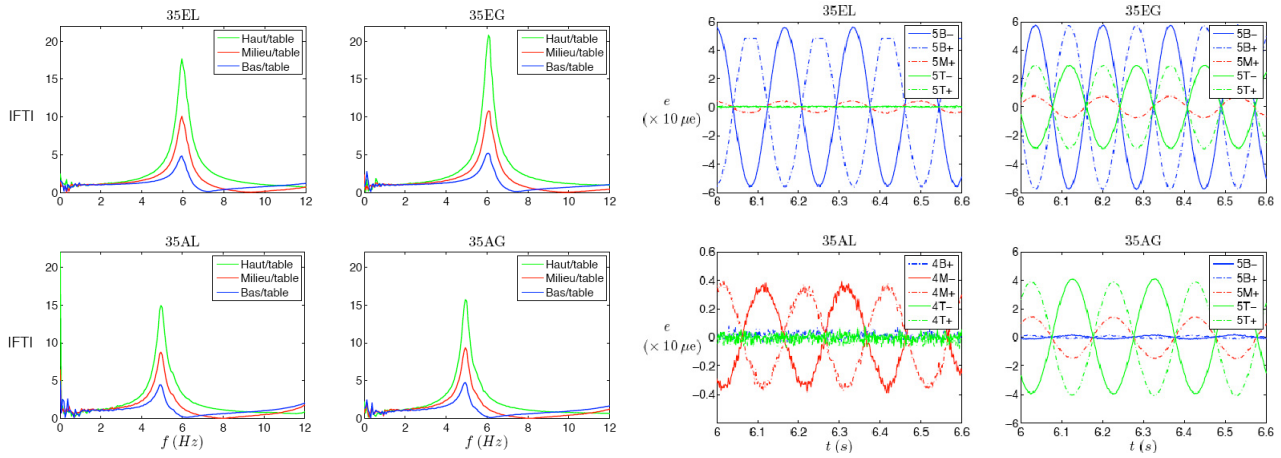

Fig. 3. Response of the sample with 35 beams tested with the four different boundary conditions. Left : Fundamental frequency identified from spectrum recorded under white noise motion. Right : Momentum in the beam evidenced by the gauge response recorded under harmonic motion at the fundamental frequency.

In Fig. 4, the fundamental mode shape and the curvature (derived from momentum measured through gauges) are compared to theoretical predictions given by the model with the same boundary conditions. For the clamped-free, clamped-translational and rotational-free boundary conditions, the homogenised model matches the experimental data (while the beam model and composite model fails to predict the experiments). For the rotational-translational conditions, the experiments departs more significantly from the theory.

Further, all these observations are similar for the configurations with 17 fibers. In the whole, the experiments are in good agreement with the theoretical model.

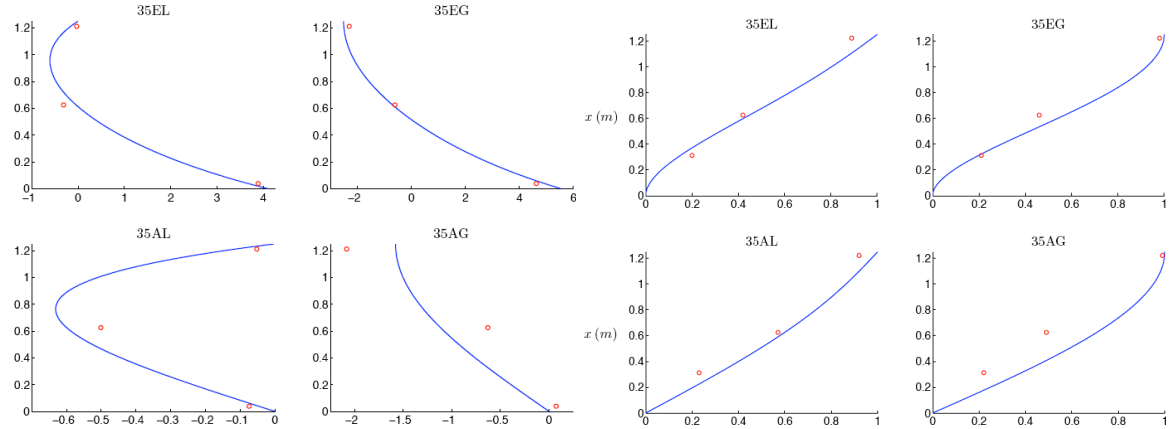

Fig. 4. Experiment (dot) versus theory (line). Comparison performed on the sample with 35 beams tested with the four different boundary conditions. Left bloc : Fundamental mode shapes related to the four boundary conditions (EL, EG on top, Al, AG on bottom). Vertical axis is the high of the pile, horizontal axis is the normalized acceleration (theoretical and extracted from the accelerometer measurements) . Right bloc : curvature related to the four boundary conditions (EL, EG on top, Al, AG on bottom). Vertical axis is the high of the pile, horizontal axis is the curvature (theoretical and extracted from the gauge measurements).

3. Urbanization effect on seismic response

E Wirgin and Bard, [9], suggested that some specific features (beatings, long duration) of the seismic motion recorded in Mexico City during the 1985 Michoacan earthquake, could be explained by the energy re-radiated in their surroundings by the buildings involved in multiple interactions. This question, investigated numerically by several authors, e.g. [10] or [11], is handle here in an theoretical/analytical manner [12,13,14]. We study the seismic response of a densely urbanized city resting on a homogeneous plane half space. The idealized city is characterized by an elementary representative block (ERB) containing a building, and the city is seen a periodic distribution of the same ERB, in the two directions of the ground surface. The buildings are taken to be linear elastic structures and the study is restricted to the effect of their first mode of oscillation. Thus, each building is described by an equivalent three degree of freedom oscillator.

3.1. Statement of the problem

Consider a Σ-periodic distribution of oscillators that lies on the top plane surface Γ of an homogeneous elastic half space (of elastic tensor C and density ρ). We study the propagation of harmonic waves of frequency $f = \omega/2\pi$, assuming a scale separation between the characteristic size l of the period Σ_0 and the wavelength in the medium, i.e.:

$$\varepsilon = 2\pi l/\lambda \ll 1$$

The wave frequency and oscillator's eigen frequencies are assumed of the same order of magnitude. The oscillators set in motion by the waves induce on Γ ($x_3 = 0$, outward normal $-e_3$) an heterogeneous distribution of stress, t.exp($i\omega t$). It is clear that, (i) at the Σ-scale, the force distribution is locally Σ-periodic, (ii) the stress distribution may also vary at the macro-scale, i.e. the wavelength scale. Following the homogenisation procedure

the variations at both scales are described by the macro-variables x and micro-variables y, with $y = \varepsilon^{-1}x$ and the physical quantities are expressed in the form of asymptotic expansions in power of ε. The local 2D periodicity of the surface forces enforces the same 2D local periodicity of the physical quantities in the medium. However, the sources of these small scale variations being located on the top surface only, it is expected that far from the boundary, the small scale variations vanish, while the large scale variations remain. Such situation can be described by introducing a boundary layer in the vicinity of the surface, [13]. The boundary layer at the soil-city interface describes the near fields radiated by each building and their multiple interactions. These assumptions lead to postulate a solution on the form defined hereafter.

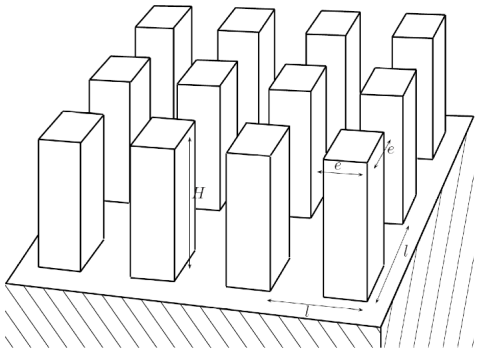

Fig. 5. Idealized city.

Far from the surface, only the macro-variables are relevant. The elastodynamics equations applies on the expanded quantities (the time dependence, $\exp(i\omega t)$ is omitted):

$$\mathbf{u}(\mathbf{x}) = \sum_{0}^{\infty} \varepsilon^i \mathbf{u}^i(\mathbf{x}) \qquad \sigma(\mathbf{x}) = \sum_{0}^{\infty} \varepsilon^i \sigma^i(\mathbf{x}) \qquad \text{with :} \qquad \sigma(\mathbf{x}) = \mathbf{C} : \mathbf{e}_{\mathbf{x}}(\mathbf{u}) \qquad \mathbf{div}_{\mathbf{x}}(\sigma) = -\rho\omega^2 \mathbf{u}$$

where u, e(u), σ, respectively denote the displacement, the strain tensor and the stress tensor. This macro-field does not match the small scale variations of the surface forces.

To match the conditions on the surface, a boundary layer (BL) field (denoted by *) is added to the macro-field. The BL field, confined near the surface, varies at both micro- and macro-scale. Hence the elastodynamics equations take the following form in the boundary layer :

$$\sigma(\mathbf{x}) + \sigma^\star(\mathbf{x}_\alpha, \mathbf{y}) = \mathbf{C} : (\varepsilon^{-1}\mathbf{e}_\mathbf{y} + \mathbf{e}_\mathbf{x})(\mathbf{u} + \mathbf{u}^\star) \qquad ; \qquad (\varepsilon^{-1}\mathbf{div}_\mathbf{y} + \mathbf{div}_\mathbf{x})(\sigma + \sigma^\star) = -\rho\omega^2(\mathbf{u} + \mathbf{u}^\star)$$

When the boundary layer plays an effective role, the surface forces t, the macro-field stress σ, and the boundary layer stress σ⋆ , are of the same order of magnitude. Thus, the expansions of the surface forces and of the BL stresses take the form :

$$\mathbf{t}(\mathbf{x}_\alpha, \mathbf{y}) = \sum_{0}^{\infty} \varepsilon^i \mathbf{t}^i(\mathbf{x}_\alpha, \mathbf{y}) \qquad \sigma^\star(\mathbf{x}_\alpha, \mathbf{y}) = \sum_{0}^{\infty} \varepsilon^i \sigma^{\star i}(\mathbf{x}_\alpha, \mathbf{y})$$

and from the definition of σ⋆ the BL motion expansion begins at the order ε:

$$\mathbf{u}^\star(\mathbf{x}_\alpha, \mathbf{y}) = \sum_{1}^{\infty} \varepsilon^i \mathbf{u}^{\star i}(\mathbf{x}_\alpha, \mathbf{y})$$

All the terms of the expansions in the boundary layer fulfill the condition of Σ_0-periodicity according to the y_α variables. Moreover, by principle :

- on Γ ($y_3 = 0$), the total stress field balances the surface forces : $-(\sigma+\sigma^\star).e_3 = t$

- far from Γ,i.e. when $y_3 \to \infty$, the total field should only presents variations according to the macro-scale. Thus the small scale variations of the BL field vanish, which leads to the condition: $\nabla_y u^\star \to 0$ $y_3 \to \infty$.

3.2. Macro-description at the leading order

The homogenisation procedure enables to define the macroscopic boundary conditions on Γ, [13]. One establishes that the zero order description is fully determined by the field $u^0(x) \equiv U^0(x)$ governed by the usual elastodynamic equation and the following boundary condition (for simplicity the index 0 is skipped) :

$$\begin{aligned} \mathbf{div_x}[\mathbf{C} : \mathbf{e_x}(\mathbf{U})] &= -\rho\omega^2\mathbf{U} \\ -[\mathbf{C} : \mathbf{e_x}(\mathbf{U})].\mathbf{e_3} &= \mathbf{T} = -|\Sigma_0|^{-1}\int_{\Sigma_0}\mathbf{t^0}\mathrm{d}s \qquad \text{on } \mathbf{x_3 = 0} \end{aligned}$$

Thus, at the leading order considered here, the surface motion is uniform on the period and the macro- field balances the *mean* surface stresses. Further, since the linear oscillators respond to the surface motion, the macro-stress T on Γ is related to the surface velocity $-i\omega U_\Gamma$ through a frequency-dependent impedance matrix Z_Γ defined by the properties of the oscillators. Finally, the leading order boundary condition states that the "oscillators layer" at the leading order acts as an equivalent impedance matrix :

$$[C : e(U)].n = -i\omega Z_\Gamma.U \quad \text{on} \quad x_3 = 0$$

To illustrate the impedance properties, consider a single oscillator located on Σ that presents a single degree-of-freedom characterised by a stiffness k, a viscous damping coefficient c and a mass m in a given direction (e.g. horizontal) so that, on this direction, the problem is scalar. The surface motion U_Γ induces a motion U_m of the mass of the oscillator. The force $|\Sigma|T$ imposed by the oscillator on Γ balances the mass inertia. Consequently

$$|\Sigma|T = (k - i\omega c)(U_m - U_\Gamma) = m\omega^2 U_m$$

Then, introducing the eigen frequency $f_o = \omega_o/2\pi$ and the damping ratio ξ (weak damping is assumed)

$$\omega_o = 2\pi f_o = \sqrt{k/m} \quad ; \quad \xi = c/2\sqrt{km} \ll 1$$

we have

$$\frac{U_m}{U_\Gamma} = \frac{1 - 2i\xi\frac{\omega}{\omega_o}}{1 - 2i\xi\frac{\omega}{\omega_o} - \frac{\omega^2}{\omega_o^2}} \quad ; \quad T = \frac{m\omega^2}{|\Sigma|}\frac{1 - 2i\xi\frac{\omega}{\omega_o}}{1 - 2i\xi\frac{\omega}{\omega_o} - \frac{\omega^2}{\omega_o^2}}U_\Gamma = -i\omega Z_\Gamma U_\Gamma$$

This last relation provides the impedance Z_Γ (in the oscillator direction). Normalized by the shear impedance $Z = \sqrt{\rho\mu} = \rho c_S$ of the elastic half space, Z_Γ is the product of a constant parameter η and of a dimensionless frequency dependent function :

$$\frac{Z_\Gamma}{Z} = -\eta\frac{(-i\frac{\omega}{\omega_o})(1 - i2\xi\frac{\omega}{\omega_o})}{1 - i2\xi\frac{\omega}{\omega_o} - \frac{\omega^2}{\omega_o^2}} \qquad \text{where} \qquad \eta = \frac{\omega_o \ell}{c_S}\frac{m}{\rho|\Sigma|\ell}$$

Parameter η is the product of two terms. First $\varepsilon_o = \omega_o l/c_S$ i.e. the scale ratio at the eigen pulsation ω_o of the oscillator. For the resonance to occur under scale separation condition, $\varepsilon_o \ll 1$. The second term is the ratio between the oscillator mass m and the mass $M\Sigma = \rho|\Sigma|l$ of the medium under one period Σ on a depth l. Hence, η is at best of the first order (in ε_o) if the resonating mass m is of the same order as $M\Sigma$. The impedance ratio Z_Γ/Z, in the low, high and resonant frequency ranges are assessed by :

$$\left|\frac{Z_\Gamma}{Z}\right|_{\omega \ll \omega_o} \simeq \left|i\frac{\omega}{\omega_o}\eta\right| \ll 1 \quad ; \quad \left|\frac{Z_\Gamma}{Z}\right|_{\omega \gg \omega_o} \simeq |-2\xi\eta| \ll 1 \quad ; \quad \left|\frac{Z_\Gamma}{Z}\right|_{\omega \to \omega_o} \simeq \left|-\frac{\eta}{2\xi}\right|$$

In quasi-static ($\omega \ll \omega_o$) or inertial ($\omega \gg \omega_o$) regime, the impedance Z_Γ is much smaller than the medium impedance Z. Consequently, the boundary condition tends to the free surface condition. Conversely, at the resonance ($\omega \to \omega_o$) the impedances ratio tends to $-\eta/2\xi$. If the oscillators are perfectly elastic ($\xi = 0$), Z_Γ/Z becomes infinite, and the surface displacement tends to zero in the direction of the oscillations: this phenomenon has the same effects as a rigid condition (in the direction of the oscillations only). For the resonant surface effect to be not negligible at the resonance under the scale separation condition, the two following inequalities have to be fullfilled necessarily: $\varepsilon_o < 1$ and $\eta/2\xi > \varepsilon_o$. This provides the two following constrains for the oscillator:

$$k < \frac{m}{M_\Sigma}\mu\ell \quad ; \quad m > 2\xi M_\Sigma$$

To sum up, the resonant surface enables to switch from quasi-free surface condition to quasi-rigid surface condition in the resonance frequency range and in the resonance direction only. Combining oscillators with different direction of oscillations open the possibility of unusual boundary condition mixing free and rigid conditions. Such situations, impossible to reach with an elastic upper layer, drastically change the usual reflection rules [16] The unconventional features of the phenomena induced by the resonant surface identified from the theory have been checked through a physical model.

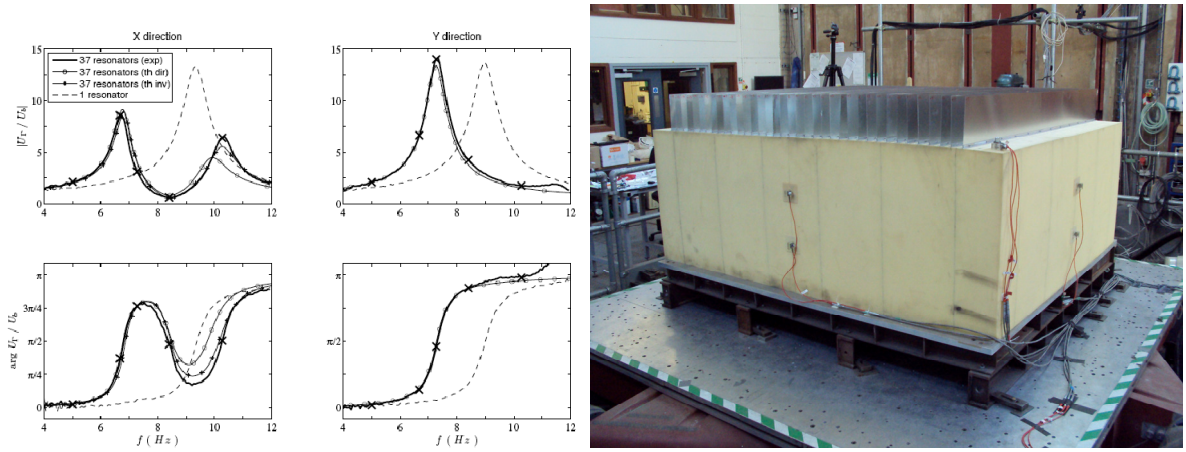

Fig. 6. Physical model of soil-city interaction. The fundamental frequency the 37 plates match that of the foam layer. Left : the specimen ; Right : Amplitude and Phase of the transfert function between the surface motion and the table motion in the resonating and non resonating directions (orthogonal and parallel to plates). Comparison between theory and experiment and with the case of a single oscillator.

3.3 Experimental validation

An experimental program has been conducted within the SERIES project [14,15]. The resonant surface is made up of 37 bending beams (made of metallic plates) resting on a soft layer made of foam (Fig. 6-a). The specimen is designed so that the oscillators' eigenfrequency match the fundamental frequency of the layer. The analysis of the response of the specimen analogue to a site-city system provide valuable information on the city effect under vertically incident SH wave. According to the trends provided by the homogenized model, the tests illustrate the expected phenomena associated to the site-city effect:

- reduced amplitude of the ground and oscillators motions in the resonating direction around the common fundamental frequency of both layer and oscillators (Fig. 6-b right), and no effect in the non- resonating direction (Fig. 6-b left),

- splitting of the resonance peak that favours beating of the signal (Fig.6-b and 7),

- increased duration of the response with slower decreasing of the coda (Fig. 7),

- change in horizontal polarisation for input SH motion oriented out of the resonating axes of the oscillators (Fig. 8). These experimental observations agree with the equivalent impedance model.

Other experiments with different configurations (5, 9, 17 identical oscillators ; two types of oscillators, periodic and non periodic distributions) demonstrate the same trends.

These theoretical and experimental results are relevant in the framework of large wavelength. Other phenomena can occur out scale separation (high frequencies). Moreover, application to strongly non- linear soil is out of scope but might be possible for weak non-linearity. Practical application may concern the design spectrum for clusters of limited number (at least 4) of nearby quasi-identical high- rise buildings in new city-blocks. Actually

multiple Soil-Structure-Interaction mechanism are usually not accounted for in design, where free surface conditions are generally assumed, as is usually valid considering a dissonance in the eigenfrequencies of the buildings and the layer. The present study raises the issue of a modification of both the soil and structures motion by these mechanisms and suggests that those local perturbations can be reduced into an effective resonant impedance for the waves and for the structures themselves.

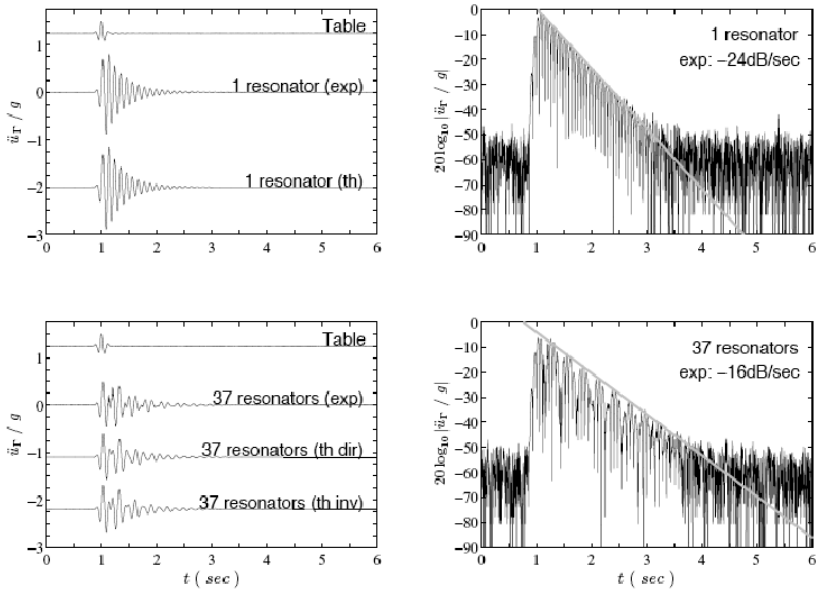

Fig. 7 Change in the time response due to the resonators. The experiments are in good agreement with the simulations performed with the homogenized model.

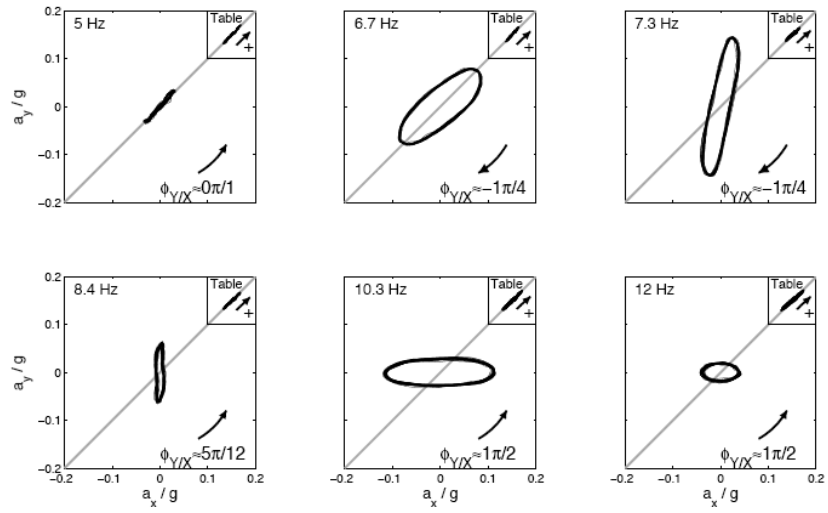

Fig. 8. Depolarization effect in the frequency range of resonance : the top motion orientation departs considerably from the table motion orientation

4. Conclusion

This work illustrates the potential of application of multi-scale approach in civil engineering. Obviously the considered configurations are over simplified compared to the reality. However, such analysis based on up-scaling, provides a first level of information on the phenomenon that occurs in the linear elastic range. This enables to identify the key parameters that governs complex phenomena as the pile group effect or multi-building interaction usually present in practice.

Acknowledgments

The Authors are pleased to thank Frederic Sallet from ENTPE/DGCB Laboratory and David Ward and Edward Skuse from the EQUALS Laboratory for their key contribution in realising the experiments in the framework of the European project Series (WP7-TA7, N0227887)

5. References

[1] Sanchez-Palencia E. (1980) Non Homogeneous Media and Vibration Theory, *Lectures Notes in Physics*, Vol. 127, Springer-Verlag, Berlin.

[2] Auriault J.L., Boutin C., Geindreau C. (2009) Homogénéisation de phénomènes couplés en milieux hétérogènes, *Mécanique et Ingénierie des Matériaux*, Hermes, Lavoisier

[3] Makris N., Gazetas G. (1992) Dynamic pile-soil-pile interaction *Earth. Engng. Struct. Dyn.* 21, pp 145-162

[4] Boutin, C., Soubestre J., (2011), Generalized inner bending continua for linear fiber reinforced materials, *Int. Journal of Solids and Structures*, 48, pp. 517-534,

[5] Soubestre J., Boutin C.(2012) Non-local dynamic behaviour of linear fiber reinforced materials, Mechanics of Materials 55, pp. 16-32

[6] Pideri C., Seppecher P. (1997), A second gradient material resulting from the homogenization of an heterogeneous linear elastic medium *Continuum Mech. and Thermodyn.* 9, pp 241-257

[7] Sudret B., De Buhan P. (1999) Modélisation multiphasique de matériaux renforcés par inclusions linéaires, *C.R.Acad.Sci.IIb.* 327,pp7-12

[8] Soubestre J., Boutin C., Dietz M.S., Dihoru L., Hans S., Ibraim E., Taylor C.A. (2012) Dynamic Behaviour of Reinforced Soils -Theoretical Modelling and Shaking Table Experiments *Geotechnical, Geological, and Earthquake Engineering* 22, pp 247-263

[9] Wirgin A., Bard P.Y. (1996), Effects of buildings on the duration and amplitude of ground motion in Mexico city, *Bull. Seism. Soc. Am.*, 86, 3, pp. 914-920.

[10] Clouteau D., Aubry D. (2001) Modification of the Ground Motion in Dense Urban Areas, *Journal of Computational Acoustics*, Vol. 9, No. 4, pp. 1659-1675

[11] Ghergu M., Ionescu I.R. (2009) Structure-Soil-Structure coupling in seismic excitation and city effect *International Journal of Engineering Science*, Vol. 47, pp. 342-354

[12] Boutin C., Roussillon P. (2004) Assessment of the Urbanization Effect on Seismic Response, *Bull. Seism. Soc. Am.*, Vol. 94, No. 1, pp. 251-268

[13] Boutin C., Roussillon P. (2006) Wave propagation in presence of oscillators on the free surface, *International Journal of Engineering Science* 4 pp180-204

[14] L. Schwan, C. Boutin, L. A. Padron, M. S. Dietz, P.-Y. Bard and C. Taylor (2016) Site-city interaction: Theoretical, numerical and experimental crossed-analysis *Geophysical Journal International* 203, pp.1694-1725

[15] C. Boutin, Schwan, L., Dietz, M. (2015) Depolarization of mechanical waves by anisotropic metasurface *Journal of Applied Physics* 117(06) 064902 8p.

[16] Schwan L., Boutin C. (2013) Unconventional wave reflection due to resonant surface *Wave Motion* 50 pp. 852-868